1 **Rapid reduction in ecosystem productivity caused by flash drought based on**

2 **decade-long FLUXNET observations**

3 Miao Zhang[a,c], Xing Yuan[b*]

4 [a]Key Laboratory of Regional Climate-Environment for Temperate East Asia

5 (RCE-TEA), Institute of Atmospheric Physics, Chinese Academy of Sciences, Beijing

6 100029, China

7 [b]School of Hydrology and Water Resources, Nanjing University of Information

8 Science and Technology, Nanjing 210044, China

9 [c]College of Earth and Planetary Sciences, University of Chinese Academy of Sciences,

10 Beijing 100049, China

13 Submitted May 7, 2020

14 Revised September 25, 2020

[*]*Corresponding author address:* Xing Yuan, School of Hydrology and Water Resources, Nanjing University of Information Science and Technology, Nanjing 210044, China E-mail: xyuan@nuist.edu.cn

Abstract. Flash drought is characterized by its rapid onset and arouses wide concerns due to its devastating impacts on the environment and society without sufficient early warnings. The increasing frequency of soil moisture flash drought in a warming climate highlights the importance of understanding its impact on terrestrial ecosystems. Previous studies investigated the vegetation dynamics during several extreme cases of flash drought, but there is no quantitative assessment on how fast the carbon fluxes respond to flash drought based on decade-long records with different climates and vegetation conditions. Here we identify soil moisture flash drought events by considering decline rate of soil moisture and the drought persistency, and detect the response of ecosystem carbon and water fluxes to soil moisture flash drought during its onset and recovery stages based on observations at 29 FLUXNET stations from croplands to forests. Corresponding to the sharp decline in soil moisture and higher VPD, gross primary productivity (GPP) drops below its normal conditions in the first 16 days and reduces to its minimum within 24 days for more than 50% of the 151 identified flash drought events, and savannas show highest sensitivity to flash drought. Water use efficiency increases for forests but decreases for cropland and savanna during the recovery stage of flash droughts. These results demonstrate the rapid responses of vegetation productivity and resistance of forest ecosystems to flash drought.

Keywords: Flash drought; GPP; Soil moisture; Water use efficiency; FLUXNET

1. Introduction

Terrestrial ecosystems play a key role in the global carbon cycle and absorb about 30% of anthropogenic carbon dioxide emissions during the past five decades (Le Quéré et al., 2018). With more climate extremes (e.g. droughts, heat waves) in a warming climate, the rate of future land carbon uptake is highly uncertain regardless of the fertilization effect of rising atmospheric carbon dioxide (Green et al., 2019; Reichstein et al., 2013; Xu et al., 2019). Terrestrial ecosystems can even turn to carbon source during extreme drought events (Ciais et al., 2005). Record-breaking drought events have caused enormous reduction of the ecosystem gross primary productivity (GPP), such as the European 2003 drought (Ciais et al., 2005; Reichstein et al., 2007), USA 2012 drought (Wolf et al., 2016), China 2013 drought (Xie et al., 2016; Yuan et al., 2016), Southern Africa 2015/16 drought (Yuan et al., 2017) and Australia Millennium drought (Banerjee et al., 2013). The 2012 summertime drought in USA was classified as flash drought with rapid intensification and insufficient early warning, which caused 26% reduction in crop yield (Hoerling et al., 2014; Otkin et al., 2016). Flash drought may only need several weeks to develop into its maximum intensity, and the rapid onset distinguishes it from traditional drought which is assumed to be a slowly evolving climate phenomenon taking several months or even years to develop (Otkin et al., 2018). Several extreme flash droughts would ultimately propagate into long-term droughts due to persistent precipitation deficits, e.g., 2012 flash drought over the USA Midwest Plain (Basara et al., 2019). Flash drought has aroused wide concerns for its unusually rapid development and detrimental effects

57 (Basara et al., 2019; Christian et al., 2019; Ford & Labosier, 2017; Nguyen et al.,

58 2019; Otkin et al., 2018a; Otkin et al., 2018b; Wang and Yuan, 2018; Yuan et al., 2015;

59 Yuan et al., 2017; Yuan et al., 2019b). Despite the increasing occurrence and clear

60 ecological impacts of flash droughts, our understanding of their impacts on carbon

61 uptake in terrestrial ecosystems remains incomplete.

62   Previous studies mainly focused on the response of vegetation to long-term

63 droughts, and found that the response time ranged from several months to years

64 through correlation analysis (Vicente-Serrano et al., 2013; Xu et al., 2018). The

65 response time of vegetation to flash droughts might be different, which requires

66 further investigation for quantification. Recent studies assessed the impact of flash

67 drought on vegetation including the 2012 central USA flash drought and the 2016 and

68 2017 northern USA flash drought. For instance, Otkin et al. (2016) used the

69 evaporative stress index (ESI) to detect the onset of the 2012 central USA flash

70 drought, and found the decline in ESI preceded the drought according to the United

71 States Drought Monitor (Svoboda et al., 2002). He et al. (2019) assessed the impacts

72 of the 2017 northern USA flash drought (which also impacted parts of southern

73 Canada) on vegetation productivity based on GOME-2 solar-induced fluorescence

74 (SIF) and satellite-based evapotranspiration in the US Northern plains. Otkin et al.

75 (2019) examined the evolution of vegetation conditions using LAI from MODIS

76 during the 2015 flash drought over the South-Central United States and found that the

77 LAI decreased after the decline of soil moisture. Besides, the 2016 flash drought over

78 U.S. northern plains also decreased agricultural production (Otkin et al., 2018b).

79   However, previous impact studies only focused on a few extreme flash drought cases

80   without explicit definition of flash drought events. As the baseline climate is changing

81   (Yuan et al., 2019b), it is necessary to systematically investigate the response of

82   terrestrial carbon and water fluxes to flash drought events based on long-term records

83   rather than one or two extreme cases.

84   In fact, there are numerous studies on the influence of drought on ecosystem

85   productivity (Ciais et al., 2005; Stocker et al., 2018; Stocker et al., 2019). It is found

86   that understanding the coupling of water-carbon fluxes during drought is the key to

87   revealing the adaptation and response mechanisms of vegetation to water stress

88   (Boese et al., 2019; Nelson et al., 2018). Water use efficiency (WUE) is the metric for

89   understanding the trade-off between carbon assimilation and water loss through

90   transpiration (Beer et al., 2009; Cowan and Farquhar, 1977; Zhou et al., 2014, 2015),

91   and it is influenced by environmental factors including atmospheric dryness and soil

92   moisture limitations (Boese et al., 2019). Although WUE has been widely studied for

93   seasonal to decadal droughts, few studies have investigated WUE during flash

94   droughts that usually occur at sub-seasonal time scale (Xie et al., 2016; Zhang et al.,

95   2019).

96   In this paper, we address the ecological impact of soil moisture flash droughts

97   through analyzing FLUXNET decade-long observations of CO_2 and water fluxes.

98   Here we consider not only the rapid onset stage of soil moisture flash droughts but

99   also the recovery stage to assess the ecological impacts. The ecological responses to

100   water stress vary under different ecosystems and drought characteristics, and the focus

101   on the soil moisture flash droughts would detect the breakdown of ecosystem

102   functioning of photosynthesis. The specific goals are to (1) examine the response of

103   carbon and water fluxes to soil moisture flash droughts from the onset to the recovery

104   stages, and (2) investigate how WUE changes during soil moisture flash drought for

105   different ecosystems. The methodology proposed by Yuan et al. (2019b) enables the

106   analysis of the flash drought with characteristics of duration, frequency, and intensity

107   in the historical observations. All the flash drought events occurred at the FLUXNET

108   stations are selected to investigate the response of carbon fluxes and WUE. More than

109   10-year records of soil moisture, carbon and water fluxes are available (Baldocchi et

110   al., 2002), which makes it possible to assess the response of vegetation to flash

111   droughts by considering different climates and ecosystem conditions.

112   **2. Data and Methods**

113   **2.1 Data**

114   FLUXNET2015 provides daily hydrometeorological variables including precipitation,

115   temperature, saturation vapor pressure deficit (VPD), soil moisture (sm), shortwave

116   radiation (SW), evapotranspiration (ET) inferred from latent heat, and carbon fluxes

117   including GPP and net ecosystem productivity (NEP). We use GPP data based on

118   night-time partitioning method (GPP_NT_VUT_REF). Considering most sites only

119   measure the surface soil moisture, here we use daily soil moisture measurements

120   mainly at the depth of 5-10 cm averaged from half-hourly data. Soil moisture

121   observations are usually averaged over multiple sensors including time domain

122   reflectometer (TDR), frequency domain reflectometer (FDR), and water content

123   reflectometer etc. However, the older devices may be replaced with newer devices at

124   certain sites, which may decrease the stability of long-term soil moisture observations

125   and the average observation error of soil moisture is $\pm$ 2%. All daily

126   hydrometeorological variables and carbon fluxes are summed to 8-day time scale to

127   study the flash drought impact. There are 34 sites from FLUXNET 2015 dataset

128   (Table 1) consisting of 8 vegetation types, where the periods of observations are no

129   less than 10 years ranging from 1996 to 2014, and the rates of missing data are lower

130   than 5%. Here we only select the FLUXNET observations including 12 evergreen

131   needleleaf forest sites (ENF), 5 deciduous broadleaf forests (DBF), 6 crop sites

132   (CROP; 5 rain-fed sites and 1 irrigated site), 3 mixed forests (MF), and 3 savannas

133   (SAV). The sites for grasslands, evergreen broadleaf forests, and shrublands are

134   excluded because there are less than 10 soil moisture flash drought events. The

135   vegetation classification is according to International Geosphere-Biosphere Program

136   (IGBP; Belward et al., 1999), where MF is dominated by neither deciduous nor

137   evergreen tree type with tree cover larger than 60% and the land tree cover is 10-30%

138   for SAV. The detailed information is listed in Table 1.

139   **2.2 Methods**

140   **2.2.1   Definition of soil moisture flash drought events**

141   The definition of soil moisture flash drought should account for both its rapid

142   intensification and the drought conditions (Otkin et al., 2018a; Yuan et al., 2019b).

143   Here we used soil moisture percentile to identify soil moisture flash drought

144   according to Yuan et al. (2019b) and Ford et al. (2017). Figure 1 shows the procedure

145   for soil moisture flash drought identification, including five criteria to identify the

146   rapid onset and recovery stages of soil moisture flash drought. 1) Soil moisture flash

147   drought starts at the middle day of the 8-day period when the 8-day mean soil

148   moisture is less than the 40th percentile, and the 8-day mean soil moisture prior to the

149   starting time should be higher than 40th percentile to ensure the transition from a

150   non-drought condition. 2) The mean decreasing rate of 8-day mean soil moisture

151   percentile should be no less than 5% per 8 days to address the rapid drought

152   intensification. 3) The 8-day mean soil moisture after the rapid decline should be less

153   than 20% in percentile, and the period from the beginning to the end of the rapid

154   decline is regarded as the onset stage of soil moisture flash drought (those within red

155   dashed line in Figure 1). 4) If the mean decreasing rate is less than 5% in percentile or

156   the soil moisture percentile starts to increase, the soil moisture flash drought enters

157   into the "recovery" stage, and the soil moisture flash drought event (as well as the

158   recovery stage) ends when soil moisture recovers to above 20th percentile (those

159   within blue dashed line in Figure 1). The recovery stage is also crucial to assess the

160   impact of soil moisture flash drought (Yuan et al., 2019b). 5) The minimum duration

161   of a flash drought event is 24 days to exclude those dry spells that last for a too short

162   period to cause any impacts.

163   At least decade-long observations of 8-day mean soil moisture are used to

164   calculate soil moisture percentile with a moving window of 8-day before and 8-day

165   after the target 8-day, resulting in at least 30 samples for deriving the cumulative

166   distribution function of soil moisture before calculating percentiles. Besides, the target

167 8-day soil moisture percentiles are only based on the target 8-day soil moisture in the

168 context of the expanded samples. For example, the soil moisture percentile of June

169 22nd in 1998 is calculated by firstly ranking June 14th, June 22nd, and June 30th soil

170 moisture in all historical years (N samples) from lowest to highest, identifying the

171 rank of soil moisture of June 22nd, 1998 (e.g., M), and obtaining the percentile as

172 M/N*100. We focus on growing seasons during April-September for sites in the North

173 Hemisphere and October-March for sites in the South Hemisphere.

174 **2.2.2   Response time of GPP to soil moisture flash drought**

175   Drought has a large influence on ecosystem productivity through altering the plant

176 photosynthesis and ecosystem respiration (Beer et al., 2010; Green et al., 2019;

177 Heimann & Reichstein, 2008; Stocker et al., 2018). GPP dominates the global

178 terrestrial carbon sink and it would decrease due to stomatal closure and non-stomatal

179 limitations like reduced carboxylation rate and reduced active leaf area index (de la

180 Motte et al., 2019) under water stress. The negative anomalies of GPP during soil

181 moisture flash drought are considered as the onset of ecological response. Here, we

182 use two response time indices to investigate the relationship between soil moisture

183 flash drought and ecological drought (Crausbay et al., 2017; Niu et al., 2018; Song et

184 al., 2018; Vicente-Serrano et al., 2013): 1) the response time of the first occurrence

185 (RT) of negative standardized GPP anomaly (SGPPA=$\frac{GPP-\mu_{GPP}}{\sigma_{GPP}}$, where μ_{GPP} and

186 σ_{GPP} are mean and standard deviation of the time series of GPP at the same dates as

187 the target 8-days for all years, which can remove the influence of seasonality. For

188 instance, all Apr 1-8 during 1996-2014 would have a μ_{GPP} and a σ_{GPP} based on a

189 climatology same as soil moisture percentile calculation which consists of March

190 24-31, Apr 1-8, and Apr 9-16 in all years, and Apr 9-16 would have another μ_{GPP}

191 and another σ_{GPP}, and so on), which is the lag time between the start of flash drought

192 and the time when SGPPA becomes negative during flash drought period; and 2) the

193 response time of occurrence of minimum SGPPA (RTmin), which is the lag time

194 between the start of flash drought and the time when SGPPA decreases to its

195 minimum values during the flash drought period. If the response time is 8 days for the

196 first occurrence of negative SGPPA, it means that the response of GPP starts at the

197 beginning of flash drought (the first time step of flash drought). Considering flash

198 drought is identified through surface soil moisture due to the availability of

199 FLUXNET data, vegetation with deeper roots may obtain water in deep soil and

200 remain healthy during flash drought. The roots vary among different vegetation types

201 and forests are assumed to have deeper roots than grasslands, which may influence the

202 response to soil moisture flash droughts.

203 **2.2.3 Water use efficiency**

204 Carbon assimilation and transpiration are coupled by stomates, and plants face a

205 tradeoff between carbon uptake through photosynthesis and water loss through

206 transpiration under the influence of water and energy availability (Boese et al., 2019;

207 Gentine et al., 2019; Huang et al., 2016; Nelson et al., 2018). WUE can be used to

208 quantify the trade-off between carbon and water cycles, which is defined as the

209 assimilated amount of carbon per unit of water loss (Peters et al., 2018). At the

210 ecosystem scale, WUE is the ratio of GPP over ET (Cowan and Farquhar, 1977).

Drought would cause stomatal closure and non-stomatal adjustments in biochemical functions thus altering the coupling between GPP and ET. Underlying WUE (uWUE) is calculated as $GPP \times \sqrt{VPD}/ET$ considering the nonlinear relationship between GPP, VPD and ET (Zhou et al., 2014). uWUE is supposed to reflect the relationship of photosynthesis-transpiration via stomatal conductance at the ecosystem level by considering the effect of VPD on WUE (Beer et al., 2009; Boese et al., 2019; Zhou et al., 2014, 2015). WUE varies under the influence of VPD on canopy conductance (Beer et al., 2009; Tang et al., 2006), whereas uWUE is considered to remove this effect and be more directly linked with the relationship between environmental conditions (e.g., soil moisture) and plant conditions (e.g., carboxylation rate; Lu et al., 2018). The standardized anomalies of WUE and uWUE are calculated the same as SGPPA, where different sites have different mean values and standard deviations for different target 8-days to remove the spatial and temporal inhomogeneity.

2.2.4   The relations between meteorological conditions and GPP

Considering the compound impacts of temperature, radiation, VPD and soil moisture on vegetation photosynthesis, the partial correlation is used to investigate the relationship between GPP and each climate factor, with the other 3 climate factors as control variables as follows:

$$r_{ij(m_1,m_2\ldots m_n)} = \frac{r_{ij(m_1,\ldots m_{n-1})} - r_{im_n(m_1,\ldots m_{n-1})} r_{jm_n(m_1,\ldots m_{n-1})}}{\sqrt{(1-r_{in(m_1,\ldots m_{n-1})}^2)(1-r_{jn(m_1,\ldots m_{n-1})}^2)}} \qquad (1)$$

where i represents GPP, j represents the target meteorological variables and $m_1, m_{2\ldots}$ and m_n represent the control meteorological variables. $r_{ij(m_1,m_2\ldots m_n)}$ is the partial correlation coefficient between i and j, and $r_{ij(m_1,\ldots m_{n-1})}$, $r_{im_n(m_1,\ldots m_{n-1})}$ and

233    $r_{jm_n(m_1,...m_{n-1})}$ are partial correlation coefficients between i and j, i and m_n, j and

234   m_n respectively under control of $m_1, m_{2...} and\ m_{n-1}$.

3. Results

3.1 Identification of flash drought events at FLUXNET stations

236   Based on FLUXNET data, we have identified 151 soil moisture flash drought

238 events with durations longer than or equal to 24 days using soil moisture observations

239 of 371 site years. Figure 2a shows the distribution of the 29 sites with different

240 vegetation types, which are mainly distributed over North America and Europe. The

241 number of soil moisture flash drought ranges from 13 to 70 events among different

242 vegetation types. There are 12 ENF sites in this study, and the number of soil moisture

243 flash droughts for ENF (70) is the most among all the vegetation types. The duration

244 for flash drought events ranges from 24 days to several months. In some extreme

245 cases, the flash droughts would develop into long-term droughts without enough

246 rainfall to alleviate drought conditions. Mean durations of soil moisture flash droughts

247 for different vegetation types range from around 30 days to 50 days (Figure 2c).

248   Figure 3 shows the meteorological conditions during different stages of soil

249 moisture flash drought including the standardized anomalies of temperature,

250 precipitation, VPD, and shortwave radiation and soil moisture percentiles. Here the

251 onset and recovery stages of flash droughts refer to certain periods characterized by

252 the soil moisture decline rates. The standardized anomalies of temperature,

253 precipitation, VPD, and shortwave and soil moisture percentiles are composited to

254 show the meteorological conditions during different stages of flash droughts. The

255   onset stage of soil moisture flash droughts mainly refers to the rapid intensification,

256   and the flash droughts may or may not develop into long-term droughts depending on

257   the deficits in precipitation. There is a slight reduction in precipitation during 8 days

258   prior to soil moisture flash drought (Figure 3b). During the onset of soil moisture

259   flash drought, soil moisture percentiles decline rapidly from nearly 50% during 8 days

260   before flash drought to 18% during onset stages (Figure 3e). The rapid drying of soil

261   moisture is always associated with a large precipitation deficits, anomalously high

262   temperature and shortwave radiation and large VPD indicate increased atmospheric

263   dryness (Ford et al., 2017; Koster et al., 2019; Wang et al., 2016), which persist until

264   the recovery stage except for shortwave radiation. The soil moisture percentiles are

265   averaged during the onset and recovery stages and the soil moisture percentiles during

266   recovery stages are slightly lower than those during onset stages (Figure 3e)

267   considering the soil moisture is not quite dry during the early period of onset stages.

268   Sufficient precipitation occurs during the 8 days after soil moisture flash droughts to

269   relieve the drought condition and soil moisture percentiles increase from 12% during

270   recovery stages to 36% during 8 days after flash droughts.

271   **3.2 Climatological statistics of the response time of GPP to flash drought**

272   By analyzing all the 151 soil moisture flash drought events across 29 FLUXNET

273   sites, we find that negative GPP anomalies occur during 81% of the soil moisture

274   flash drought events. Figure 4 shows the probability distributions of the response time

275   of GPP to soil moisture flash drought as determined by soil moisture reductions for

276   the first occurrence of negative SGPPA, the minimum negative value of SGPPA and

the minimum soil moisture percentiles for different vegetation types, respectively. To

reduce the uncertainty due to small sample sizes, only the results for vegetation types

(SAV, CROP, MF, DBF, ENF) with more than 10 flash drought events are shown. For

soil moisture flash droughts from all vegetation types, the first occurrences of

negative SGPPA are concentrated during the first 24 days, and GPP starts to respond

to soil moisture flash drought within 16 days for 57% flash droughts (Figures 4a-e).

The occurrences of minimum value of SGPPA rise sharply at the beginning of soil

moisture flash drought, and reach the peak during 17-24 days, and then slow down

(Figures 4f-j), which is similar to the decline in soil moisture. Although the first

occurrences of negative SGPPA mainly occur in the onset stage, GPP would continue

to decrease in the recovery stages for 60% of soil moisture flash drought events.

Different types of vegetation including herbaceous plants and woody plants all react

to soil moisture flash drought in the early stage (Figures 4a-e). Among them, SAV

shows the fastest reaction to water stress (Figures 4a and 4f), and the RT is within 8

days for 63% events, suggesting that SAV responds concurrently with soil moisture

flash drought onset. Ultimately, 88% events for SAV show reduced vegetation

photosynthesis. The result is consistent with previous studies regarding the strong

response of semi-arid ecosystems to water availability (Gerken et al., 2019;

Vicente-Serrano et al., 2013; Zeng et al., 2018), and the decline in GPP for SAV is

related to isohydric behaviors during soil moisture drought and higher VPD, through

closing stomata to decrease water loss as transpiration and carbon assimilation

(Novick et al., 2016; Roman et al., 2015). For ENF, only 27% of soil moisture flash

299 droughts cause the negative SGPPA during the first 8 days. When RT is within 40

300 days, the cumulative frequencies range from 74% to 88% among different vegetation

301 types. The response frequency of RTmin and the response time of minimum soil

302 moisture percentiles are quite similar, although there are discrepancies among the

303 patterns of the response frequency for different vegetation types. The response

304 frequency of RTmin for SAV increases sharply during 17-24 days of soil moisture

305 flash droughts (Figure 4f). GPP is derived from direct eddy covariance observations

306 of NEP and nighttime terrestrial ecosystem respiration, and temperature-fitted

307 terrestrial ecosystem respiration during daytime. The response of NEP to flash

308 droughts shows the compound effects of vegetation photosynthesis and ecosystem

309 respiration. In terms of RT, the response of NEP is slower than GPP for SAV, but is

310 quicker for DBF and ENF (Figure 5). The discrepancies between NEP and SM in

311 terms of RTmin are more obvious than those between GPP and SM, and the RTmin of

312 NEP is much shorter than the RTmin of soil moisture especially for DBF and ENF,

313 which may be related to the increase of ecosystem respiration (Figures 5 i and j).

314 Figure 6 shows the temporal changes of SGPPA and soil moisture percentiles

315 during 8 days before soil moisture flash droughts and during the first 24 days of the

316 droughts. During 8 days before flash droughts, there is nearly no obvious decline for

317 SGPPA, while SAV, DBF and ENF shows small increase in GPP. The decline in

318 SGPPA is more significant during the first 9-24 days of soil moisture flash droughts

319 for different vegetation types, and SGPPA for SAV and CROP show quicker decline

320 even during the first 8 days of soil moisture flash droughts. The decline rates in soil

321   moisture are mainly concentrated within the first 16 days of flash droughts. There are

322   various lag times for the response of GPP to the decline in soil moisture among

323   different vegetation.

324   **3.3 The coupling between carbon and water fluxes under soil moisture stress**

325   Figure 7 shows the standardized anomalies of WUE and uWUE and their

326   components for different ecosystems during 8 days before and after soil moisture

327   flash droughts and the onset and recovery stages. Here, we select 81% of soil moisture

328   flash drought events with GPP declining down to its normal conditions to analyze the

329   interactions between carbon and water fluxes, while GPP during the remaining 19%

330   of soil moisture flash drought events may stay stable and is less influenced by drought

331   conditions. During 8 days before soil moisture flash drought, WUE and uWUE are

332   generally close to the climatology (Figure 7a) and there are no significant changes in

333   GPP, ET, and $ET/\sqrt{VPD}$ (Figures 7e and 7i). However, the median value of SGPPA

334   for SAV is positive (Figure 7e). WUE is stable during the onset stage, whereas uWUE

335   increases for all ecosystems except for CROP (Figure 7b). For CROP, both GPP and

336   ET decrease, and the decline in WUE is related with a greater reduction in GPP

337   relative to ET (Figure 7f and 7j). The positive anomalies of uWUE are correlated with

338   decrease in $ET/\sqrt{VPD}$ mainly induced by the high VPD. Increasing VPD and

339   deficits in soil moisture would decrease canopy conductance (Grossiord et al., 2020)

340   but not GPP for MF and ENF. During the onset stage, GPP and ET reduce only for

341   SAV, and CROP, and DBF, and the magnitudes of GPP and ET reduction are highest

342   for SAV. ET is close to normal conditions for MF, DBF, and ENF, thus enhancing the

343 drying rate of soil moisture with less precipitation supply during the onset stage. But

344 during recovery stage of soil moisture flash drought, GPP and ET show significant

345 reductions except for MF (Figures 7g and 7k), and the responses of WUE and uWUE

346 are different between herbaceous plants (SAV and CROP) and forests (MF, DBF, and

347 ENF), where WUE and uWUE decrease significantly for SAV and CROP but increase

348 slightly for forests (Figure 7c). The decrease in uWUE for SAV and CROP during

349 recovery stages indicates that SAV and CROP are likely brown due to carbon

350 starvation caused by the significant decrease in stomatal conductance (McDowell et

351 al., 2008). The decrease in GPP during recovery stage is not only related to the

352 reduction in canopy conductance, but also the decrease in uWUE under drought for

353 SAV and CROP which is possibly influenced by suppressed state of enzyme and

354 reduced mesophyll conductance (Flexas et al., 2012). However, the positive

355 anomalies of uWUE for DBF and ENF during the recover stage imply that the decline

356 in GPP mainly results from the stomata closure. ET starts to decrease during the

357 recovery stage due to the limitation of water availability, and the decreasing ET also

358 reflects the enhanced water stress for vegetation during the recovery stage. The

359 average soil moisture conditions are 12% in percentile for recovery stage but 18% for

360 onset stage. So, drier soil moisture in the recovery stage exacerbates ecological

361 response. Figure 7c also shows the higher WUE and uWUE for forests, which

362 indicates their higher resistance to flash drought than herbaceous plants during

363 recovery stage. During 8 days after flash drought, the standardized anomalies of

364 uWUE are still positive for forests, whereas SGPPA and ET are both lower than the

365   climatology for all ecosystems. The ecological negative effect would persist after the

366   soil moisture flash drought.

3.4 The impact of climate factors on GPP during soil moisture flash drought

368   Figure 8 shows the partial correlation coefficients between standardized

369   anomalies of GPP and meteorological variables and soil moisture percentiles during

370   different stages of soil moisture flash droughts. The correlation between climate

371   factors and GPP is not statistically significant during 8 days before soil moisture flash

372   droughts. During onset stages of soil moisture flash droughts, the partial correlation

373   coefficients between SGPPA and soil moisture percentiles are 0.44, 0.49 and 0.29,

374   respectively for SAV, CROP, and ENF ($p < 0.05$). Besides, shortwave radiation is

375   positively correlated with SGPPA for MF, DBF, and EBF (Figure 8b) during onset

376   stages and the positive anomalies of shortwave radiation could partially offset the loss

377   of vegetation photosynthesis due to the deficits in soil moisture. SGPP is also

378   positively correlated with temperature during onset stages for SAV and DBF. The

379   partial correlation coefficients between SGPPA and VPD are -0.53 and -0.22

380   respectively for DBF and ENF, and the higher VPD would further decrease GPP

381   during onset stages. The influence of VPD on GPP is much more significant during

382   recovery stages and 8 days after. SGPPA is positively correlated with soil moisture

383   and negatively with VPD for SAV both during recovery stages and 8 days after.

4. Discussion

385   Previous studies detected the vegetation response for a few extreme drought cases

386   without a specific definition of flash drought from a climatological perspective (Otkin

387   et al., 2016; He et al., 2019). Moreover, less attention has been paid to the coupling

388   between carbon and water fluxes during soil moisture flash drought events. This study

389   investigates the response of carbon and water fluxes to soil moisture flash drought

390   based on decade-long FLUXNET observations during different stages of flash

391   droughts. The responses vary across different phases of flash drought, and different

392   ecosystems have different responses, which provide implications for eco-hydrological

393   modeling and prediction. Besides, the influence of different climate factors including

394   VPD and soil moisture also differs during different stages of soil moisture flash

395   droughts.

396   **4.1 The responses of carbon and water fluxes to flash droughts**

397   Based on 151 soil moisture flash drought events identified using soil moisture

398   from decade-long FLUXNET observations, the response of GPP to flash drought is

399   found to be quite rapid. For more than half of the 151 soil moisture flash drought

400   events, the GPP drops below its normal conditions during the first 16 days and

401   reaches its maximum reduction within 24 days. Due to the influence of ecosystem

402   respiration, the responses of NEP for DBF and ENF to flash droughts are much

403   quicker than GPP, implying that the sensitivity of ecosystem respiration is less than

404   that of vegetation photosynthesis (Granier et al., 2007). Eventually, 81% of soil

405   moisture flash drought events cause declines in GPP. During the drought period,

406   plants would close their stomata to minimize water loss through decreasing canopy

407   conductance, which in turn leads to a reduction in carbon uptake. The soil moisture

408   flash droughts are always accompanied by high temperature and VPD. Through

409 partial correlation analysis, positive anomalies in VPD and the deficits in soil

410 moisture would both decrease the rate of photosynthesis. High VPD further reduces

411 canopy conductance to minimize water loss at the cost of reducing photosynthesis

412 during soil moisture flash drought (Grossiord et al., 2020). The suppression of GPP

413 and ET is more obvious for flash drought recovery stage determined by soil moisture

414 than the onset stage. The discrepancy of GPP responses between different phases of

415 soil moisture flash drought may result from 1) soil moisture conditions which are

416 drier during the recovery stage, and 2) the damaged physiological functioning for

417 specific vegetation types. The anomalies of uWUE for ecosystems are always positive

418 or unchanged during soil moisture flash drought except for croplands and savannas

419 during recovery stage. The decrease in canopy conductance would limit

420 photosynthetic rate, however, the increase of uWUE may indicate adaptative

421 regulations of ecosystem physiology which is consistent with Beer et al. (2009).

422 uWUE is higher than WUE during onset stage of soil moisture flash drought, which is

423 due to the decreased conductance under increased VPD. However, there is no obvious

424 difference between WUE and uWUE during recovery stage, which indicates that

425 photosynthesis is less sensitive to stomatal conductance and may be more correlated

426 with limitations of biochemical capacity (Flexas et al., 2012; Grossiord et al., 2020).

427 During 8 days after the soil moisture flash drought, the anomalies of GPP and ET are

428 still negative, indicating that the vegetation does not recover immediately after the

429 soil moisture flash drought. The legacy effects of flash droughts may be related to the

430 vegetation and climate conditions (Barnes et al., 2016; Kannenberg et al., 2020).

431   This study is based on the sites that are mainly distributed over North America

432   and Europe. It is necessary to investigate the impact of flash drought on vegetation

433   over other regions with different climates and vegetation conditions. In addition, this

434   study used in-situ surface soil moisture at FLUXNET stations to detect vegetation

435   response due to the lack of soil moisture observations at deep soil layers. There would

436   be more significant ecological responses to flash drought identified through using

437   root-zone soil moisture because of its close link with vegetation dynamics. Due to the

438   limitation of FLUXNET soil moisture measurements, here we used soil moisture

439   observations mainly at the depths of 5 to 10 cm. We also analyzed the response of

440   GPP to flash drought identified by 0.25-degree ERA5 soil moisture reanalysis data at

441   the depths of 7cm and 1m. The response of GPP to flash droughts identified by

442   FLUXNET surface soil moisture are quite similar to those identified by ERA5 soil

443   moisture at the depth of 1m (not shown). There are less GPP responses to flash

444   droughts identified by ERA5 surface soil moisture. Although we select the ERA5 grid

445   cell that is closest to the FLUXNET site and use the ERA5 soil moisture data over the

446   same period as the FLUXNET data, we should acknowledge that the gridded ERA5

447   data might not be able to represent the soil moisture conditions as well as flash

448   droughts at in-situ scale due to strong heterogeneity of land surface. Therefore, the

449   in-situ surface soil moisture from FLUXNET is useful to identify flash droughts

450   compared with reanalysis soil moisture, although the in-situ root-zone soil moisture

451   would be better.

452   **4.2 Variation in ecological responses across vegetation types**

453   The responses of GPP, ET and WUE to soil moisture flash drought vary among

454   different vegetation types. The decline in GPP and ET only occurs across croplands

455   and savannas during onset stage. For most forests, the deterioration of photosynthesis

456   and ET appears during the recovery stage with higher WUE and uWUE. For CROP

457   and SAV, both WUE and uWUE decrease during the recovery stage and they may be

458   brown due to reduced photosynthesis. The positive anomalies of WUE and uWUE for

459   forests suggest that their deeper roots can obtain more water than grasslands during

460   flash drought. Xie et al. (2016) pointed out that WUE and uWUE for a subtropical

461   forest increased during the 2013 summer drought in southern China. The increased

462   WUE in forest sites and unchanged WUE in grasslands were also found in other

463   studies for spring drought (Wolf et al., 2013). In general, herbaceous plants are more

464   sensitive to flash drought than forests, especially for savannas. The correlation

465   between soil moisture and GPP is more significant for SAV, CROP, and ENF during

466   onset stages of flash droughts, which is consistent with the strong response to water

467   availability of SAV and CROP (Gerken et al., 2019). SAV is more isohydric than

468   forests and would reduce stomatal conductance immediately to prohibit water loss

469   that further exacerbates drought (Novick et al., 2016; Roman et al., 2015). However,

470   almost all vegetation types show high sensitivity to VPD during the recovery stage of

471   flash droughts.

472   **4.3 Potential implications for ecosystem modelling**

473   The study reveals the profound impact of soil moisture flash droughts on

474   ecosystem through analyzing eddy covariance observations. It is found that the

475 responses of carbon and water exchanges are quite distinguishing for forests and

476 herbaceous plants. For the ecosystem modeling, the response of stomatal conductance

477 under soil moisture stress has been addressed in previous studies (Wilson et al., 2000),

478 but there still exists deficiency to capture the impacts of water stress on carbon uptake

479 (Keenan et al., 2009), which is partly due to the different responses across species.

480 Incorporating physiological adaptations to drought in ecosystem modeling especially

481 for forests would improve the simulation of the impact of drought on the terrestrial

482 ecosystems.

483 **5. Conclusion**

484   This study presents how carbon and water fluxes respond to soil moisture flash

485 drought during 8 days before flash droughts, onset and recovery stages, and 8 days

486 after flash droughts through analyzing decade-long observations from FLUXNET.

487 Ecosystems show high sensitivity of GPP to soil moisture flash drought especially for

488 savannas, and GPP starts to respond to soil moisture flash droughts within 16 days for

489 more than half of the flash drought events under the influence of the deficit in soil

490 moisture and higher VPD. However, the responses of WUE and uWUE vary across

491 vegetation types. Positive WUE and uWUE anomalies for forests during the recovery

492 stage indicate the resistance to soil moisture flash drought through non-stomatal

493 regulations, whereas WUE and uWUE decrease for croplands and savannas during the

494 recovery stage. For now, the main concern about the ecological impact of soil

495 moisture flash drought is concentrated on the period of flash drought and the legacy

496 effects of flash drought are not involved. It still needs more efforts to study the

subsequent effects of soil moisture flash droughts which would contribute to assessing the accumulated ecological impacts of flash drought. Nevertheless, this study highlights the rapid response of vegetation productivity to soil moisture dynamics at sub-seasonal timescale, and different responses of water use efficiency across ecosystems during the recovery stage of soil moisture flash droughts, which complements previous studies on the sensitivity of vegetation to extreme drought at longer time scale. Understanding the response of carbon fluxes and the coupling between carbon and water fluxes to drought, especially considering the effects of climate change and human interventions (Yuan et al., 2020), might help assessing the resistance and resilience of vegetation to drought.

Acknowledgements

The authors thank two anonymous reviewers for their helpful comments, and thank Dr. Zhenzhong Zeng for his constructive suggestions. This work was supported by National Natural Science Foundation of China (41875105), National Key R&D Program of China (2018YFA0606002) and the Startup Foundation for Introducing Talent of NUIST. The data used in this study are all from FLUXNET 2015 (https://fluxnet.fluxdata.org/data/fluxnet2015-dataset/).

Data availability statement

Carbon fluxes and hydrometeorological variables from FLUXNET2015 are available through https://fluxnet.fluxdata.org/data/fluxnet2015-dataset/.

References

Atjay, G. L., Ketner, P. and Duvigneaud, P.: Terrestrial primary production and phytomass, in The Global Carbon Cycle: SCOPE 13, John Wiley, Hoboken, N. J., 129–182, 1979

Baldocchi, D., Wilson, K., Valentini, R., Law, B., Munger, W., Davis, K., Wofsy, S., Pilegaard, K., Goldstein, A., Falge, E., Vesala, T., Hollinger, D., Running, S., Fuentes, J., Katul, G., Gu, L., Verma, S., Paw, K. T., Malhi, Y., Anthoni, P., Oechel, W., Schmid, H. P., Bernhofer, C., Meyers, T., Evans, R., Olson, R. and Lee, X.: FLUXNET: A New Tool to Study the Temporal and Spatial Variability of Ecosystem–Scale Carbon Dioxide, Water Vapor, and Energy Flux Densities, Bull. Am. Meteorol. Soc., 82(11), 2415–2434, https://doi.org/10.1175/1520-0477, 2002.

Banerjee, O., Bark, R., Connor, J. and Crossman, N. D.: An ecosystem services approach to estimating economic losses associated with drought, Ecol. Econ., 91, 19–27, https://doi.org/10.1016/j.ecolecon.2013.03.022, 2013.

Barnes, M. L., Moran, M. S., Scott, R. L., Kolb, T. E., Ponce-Campos, G. E., Moore, D. J. P., Ross, M. A., Mitra, B. and Dore, S.: Vegetation productivity responds to sub-annual climate conditions across semiarid biomes, Ecosphere, 7(5), 1–20, https://doi.org/10.1002/ecs2.1339, 2016

Basara, J. B., Christian, J. I., Wakefield, R. A., Otkin, J. A., Hunt, E. H. H. and Brown, D. P.: The evolution, propagation, and spread of flash drought in the Central United States during 2012, Environ. Res. Lett., 14(8),

541   https://doi.org/10.1088/1748-9326/ab2cc0, 2019.

542 Belward, A. S., Estes, J. E., and Kline, K. D.: The igbp-dis global 1-km land-cover

543   data set discover: A project overview. Photogrammc Eng Rem S, 65(9):1013–

544   1020, 1999

545 Beer, C., Ciais, P., Reichstein, M., Baldocchi, D., Law, B. E., Papale, D., Soussana, J.

546   F., Ammann, C., Buchmann, N., Frank, D., Gianelle, D., Janssens, I. A., Knohl,

547   A., Köstner, B., Moors, E., Roupsard, O., Verbeeck, H., Vesala, T., Williams, C.

548   A. and Wohlfahrt, G.: Temporal and among-site variability of inherent water use

549   efficiency at the ecosystem level, Global Biogeochem. Cycles, 23(2), 1–13,

550   https://doi.org/10.1029/2008GB003233, 2009.

551 Beer, C., Reichstein, M., Tomelleri, E., Ciais, P., Jung, M., Carvalhais, N., Rödenbeck,

552   C., Arain, M. A., Baldocchi, D., Bonan, G. B., Bondeau, A., Cescatti, A., Lasslop,

553   G., Lindroth, A., Lomas, M., Luyssaert, S., Margolis, H., Oleson, K. W.,

554   Roupsard, O., Veenendaal, E., Viovy, N., Williams, C., Woodward, F. I. and

555   Papale, D.: Terrestrial gross carbon dioxide uptake: Global distribution and

556   covariation with climate, Science, 329(5993), 834–838,

557   https://doi.org/10.1126/science.1184984, 2010.

558 Boese, S., Jung, M., Carvalhais, N., Teuling, A. J. and Reichstein, M.: Carbon-water

559   flux coupling under progressive drought, Biogeosciences, 16(13), 2557–2572,

560   https://doi.org/10.5194/bg-16-2557-2019, 2019.

561 Cowan, I. R. and Farquhar, G. D.: Stomatal function in relation to leaf metabolism

562   and environment, in Integration of Activity in the Higher Plant, edited by D. H.

Jennings, Cambridge Univ. Press, Cambridge, U. K., 471–505, 1977

Christian, J. I., Basara, J. B., Otkin, J. A., Hunt, E. D., Wakefield, R. A., Flanagan, P. X. and Xiao, X.: A methodology for flash drought identification: Application of flash drought frequency across the United States, J. Hydrometeorol., 20(5), 833–846, https://doi.org/10.1175/JHM-D-18-0198.1, 2019.

Ciais, P., Reichstein, M., Viovy, N., Granier, A., Ogée, J., Allard, V., Aubinet, M., Buchmann, N., Bernhofer, C., Carrara, A., Chevallier, F., De Noblet, N., Friend, A. D., Friedlingstein, P., Grünwald, T., Heinesch, B., Keronen, P., Knohl, A., Krinner, G., Loustau, D., Manca, G., Matteucci, G., Miglietta, F., Ourcival, J. M., Papale, D., Pilegaard, K., Rambal, S., Seufert, G., Soussana, J. F., Sanz, M. J., Schulze, E. D., Vesala, T. and Valentini, R.: Europe-wide reduction in primary productivity caused by the heat and drought in 2003, Nature, 437(7058), 529–533, https://doi.org/10.1038/nature03972, 2005.

Crausbay, S. D., Ramirez, A. R., Carter, S. L., Cross, M. S., Hall, K. R., Bathke, D. J., Betancourt, J. L., Colt, S., Cravens, A. E., Dalton, M. S., Dunham, J. B., Hay, L. E., Hayes, M. J., McEvoy, J., McNutt, C. A., Moritz, M. A., Nislow, K. H., Raheem, N. and Sanford, T.: Defining ecological drought for the twenty-first century, Bull. Am. Meteorol. Soc., 98(12), 2543–2550, https://doi.org/10.1175/BAMS-D-16-0292.1, 2017.

de la Motte, L. G., Beauclaire, Q., Heinesch, B., Cuntz, M., Foltýnová, L., Šigut, L., Kowalska, N., Manca, G., Ballarin, I. G., Vincke, C., Roland, M., Ibrom, A., Lousteau, D., Siebicke, L. and Longdoz, B.: Non-stomatal processes reduce

gross primary productivity in temperate forest ecosystems during severe edaphic

drought, Philos. Trans. R. Soc. B, https://doi.org/10.1098/RSTB-2019-0527,

2019.

Flexas, J., Barbour, M. M., Brendel, O., Cabrera, H. M., Carriquí, M., Díaz-Espejo, A.,

Douthe, C., Dreyer, E., Ferrio, J. P., Gago, J., Gallé, A., Galmés, J., Kodama, N.,

Medrano, H., Niinemets, Ü., Peguero-Pina, J. J., Pou, A., Ribas-Carbó, M.,

Tomás, M., Tosens, T. and Warren, C. R.: Mesophyll diffusion conductance to

CO2: An unappreciated central player in photosynthesis, Plant Sci., 193–194,

70–84, https://doi.org/10.1016/j.plantsci.2012.05.009, 2012.

Ford, T. W. and Labosier, C. F.: Meteorological conditions associated with the onset

of flash drought in the Eastern United States, Agric. For. Meteorol., 247(April),

414–423, https://doi.org/10.1016/j.agrformet.2017.08.031, 2017.

Ford, T. W., McRoberts, D. B., Quiring, S. M. and Hall, R. E.: On the utility of in situ

soil moisture observations for flash drought early warning in Oklahoma, USA,

Geophys. Res. Lett., 42(22), https://doi.org/10.1002/2015GL066600, 2015.

Granier, A., Reichstein, M., Bréda, N., Janssens, I. A., Falge, E., Ciais, P., Grünwald,

T., Aubinet, M., Berbigier, P., Bernhofer, C., Buchmann, N., Facini, O., Grassi,

G., Heinesch, B., Ilvesniemi, H., Keronen, P., Knohl, A., Köstner, B., Lagergren,

F., Lindroth, A., Longdoz, B., Loustau, D., Mateus, J., Montagnani, L., Nys, C.,

Moors, E., Papale, D., Peiffer, M., Pilegaard, K., Pita, G., Pumpanen, J., Rambal,

S., Rebmann, C., Rodrigues, A., Seufert, G., Tenhunen, J., Vesala, T. and Wang,

Q.: Evidence for soil water control on carbon and water dynamics in European

607   forests during the extremely dry year: 2003, Agric. For. Meteorol., 143(1–2),

608   123–145, https://10.1016/j.agrformet.2006.12.004, 2007.

609 Gentine, P., Green, J. K., Guérin, M., Humphrey, V., Seneviratne, S. I., Zhang, Y. and

610   Zhou, S.: Coupling between the terrestrial carbon and water cycles - A review,

611   Environ. Res. Lett., 14(8), https://10.1088/1748-9326/ab22d6, 2019.

612 Gerken, T., Ruddell, B. L., Yu, R., Stoy, P. C. and Drewry, D. T.: Robust observations

613   of land-to-atmosphere feedbacks using the information flows of FLUXNET,

614   Clim. Atmos. Sci., 2(37), https://doi.org/10.1038/s41612-019-0094-4, 2019.

615 Green, J. K., Seneviratne, S. I., Berg, A. M., Findell, K. L., Hagemann, S., Lawrence,

616   D. M. and Gentine, P.: Large influence of soil moisture on long-term terrestrial

617   carbon uptake, Nature, 565(7740), 476–479,

618   https://doi.org/10.1038/s41586-018-0848-x, 2019.

619 Grossiord, C., Buckley, T. N., Cernusak, L. A., Novick, K. A., Poulter, B., Siegwolf, R.

620   T. W., Sperry, J. S. and McDowell, N. G.: Plant responses to rising vapor

621   pressure deficit, New Phytol., https://doi.org/10.1111/nph.16485, 2020.

622 He, M., Kimball, J. S., Yi, Y., Running, S., Guan, K., Jensco, K., Maxwell, B. and

623   Maneta, M.: Impacts of the 2017 flash drought in the US Northern plains

624   informed by satellite-based evapotranspiration and solar-induced fluorescence,

625   Environ. Res. Lett., 14(7), 074019, https://doi.org/10.1088/1748-9326/ab22c3,

626   2019.

627 Heimann, M. and Reichstein, M.: Terrestrial ecosystem carbon dynamics and climate

628   feedbacks, Nature, 451(7176), 289–292, https://doi.org/10.1038/nature06591,

629   2008.

630   Hoerling, M., Eischeid, J., Kumar, A., Leung, R., Mariotti, A., Mo, K., Schubert, S.

631   and Seager, R.: Causes and predictability of the 2012 great plains drought, Bull.

632   Am.   Meteorol.   Soc.,   95(2),   269–282,

633   https://doi.org/10.1175/BAMS-D-13-00055.1, 2014.

634   Huang, M., Piao, S., Zeng, Z., Peng, S., Ciais, P., Cheng, L., Mao, J., Poulter, B., Shi,

635   X., Yao, Y., Yang, H. and Wang, Y.: Seasonal responses of terrestrial ecosystem

636   water-use efficiency to climate change, Glob. Chang. Biol., 22(6), 2165–2177,

637   https://doi.org/10.1111/gcb.13180, 2016.

638   Keenan, T., García, R., Friend, A. D., Zaehle, S., Gracia, C. and Sabate, S.: Improved

639   understanding of drought controls on seasonal variation in mediterranean forest

640   canopy CO2 and water fluxes through combined in situ measurements and

641   ecosystem   modelling,   Biogeosciences,   6(8),   1423–1444,

642   https://doi.org/10.5194/bg-6-1423-2009, 2009.

643   Koster, R. D., Schubert, S. D., Wang, H., Mahanama, S. P. and DeAngelis, A. M.:

644   Flash Drought as Captured by Reanalysis Data: Disentangling the Contributions

645   of Precipitation Deficit and Excess Evapotranspiration, J. Hydrometeorol., 20(6),

646   1241–1258, https://doi.org/10.1175/jhm-d-18-0242.1, 2019.

647   Kannenberg, S. A., Schwalm, C. R. and Anderegg, W. R. L.: Ghosts of the past: how

648   drought legacy effects shape forest functioning and carbon cycling, Ecol. Lett.,

649   ele.13485, https://doi.org/10.1111/ele.13485, 2020.

650   McDowell, N., Pockman, W. T., Allen, C. D., Breshears, D. D., Cobb, N., Kolb, T.,

651   Plaut, J., Sperry, J., West, A., Williams, D. G. and Yepez, E. A.: Mechanisms of

652   plant survival and mortality during drought: Why do some plants survive while

653   others succumb to drought?, New Phytol., 178(4), 719–739,

654   https://doi.org/10.1111/j.1469-8137.2008.02436.x, 2008.

655 Novick, K. A., Ficklin, D. L., Stoy, P. C., Williams, C. A., Bohrer, G., Oishi, A. C.,

656   Papuga, S. A., Blanken, P. D., Noormets, A., Sulman, B. N., Scott, R. L., Wang,

657   L. and Phillips, R. P.: The increasing importance of atmospheric demand for

658   ecosystem water and carbon fluxes, , 1(September), 1–5,

659   https://doi.org/10.1038/NCLIMATE3114, 2016.

660 Nelson, J. A., Carvalhais, N., Migliavacca, M., Reichstein, M. and Jung, M.:

661   Water-stress-induced breakdown of carbon-water relations: Indicators from

662   diurnal FLUXNET patterns, Biogeosciences, 15(8), 2433–2447,

663   https://doi.org/10.5194/bg-15-2433-2018, 2018.

664 Nguyen, H., Wheeler, M. C., Otkin, J. A., Cowan, T., Frost, A. and Stone, R.: Using

665   the evaporative stress index to monitor flash drought in Australia, Environ. Res.

666   Lett., 14(6), https://doi.org/10.1088/1748-9326/ab2103, 2019.

667 Niu, J., Chen, J., Sun, L. and Sivakumar, B.: Time-lag effects of vegetation responses

668   to soil moisture evolution: a case study in the Xijiang basin in South China,

669   Stoch. Environ. Res. Risk Assess., 32(8), 2423–2432,

670   https://doi.org/10.1007/s00477-017-1492-y, 2018.

671 Otkin, J. A., Anderson, M. C., Hain, C., Mladenova, I. E., Basara, J. B. and Svoboda,

672   M.: Examining Rapid Onset Drought Development Using the Thermal Infrared–

Based Evaporative Stress Index, J. Hydrometeorol., 14(4), 1057–1074, https://doi.org/10.1175/JHM-D-12-0144.1, 2013.

Otkin, J. A., Anderson, M. C., Hain, C., Svoboda, M., Johnson, D., Mueller, R., Tadesse, T., Wardlow, B. and Brown, J.: Assessing the evolution of soil moisture and vegetation conditions during the 2012 United States flash drought, Agric. For. Meteorol., 218–219, 230–242, https://doi.org/10.1016/j.agrformet.2015.12.065, 2016.

Otkin, J. A., Svoboda, M., Hunt, E. D., Ford, T. W., Anderson, M. C., Hain, C. and Basara, J. B.: Flash droughts: A review and assessment of the challenges imposed by rapid-onset droughts in the United States, Bull. Am. Meteorol. Soc., 99(5), 911–919, https://doi.org/10.1175/BAMS-D-17-0149.1, 2018a.

Otkin, J. A., Haigh, T., Mucia, A., Anderson, M. C. and Hain, C.: Comparison of Agricultural Stakeholder Survey Results and Drought Monitoring Datasets during the 2016 U.S. Northern Plains Flash Drought, Weather. Clim. Soc., 10(4), 867–883, https://doi.org/10.1175/wcas-d-18-0051.1, 2018b.

Otkin, J. A., Zhong, Y., Hunt, E. D., Basara, J., Svoboda, M., Anderson, M. C. and Hain, C.: Assessing the Evolution of Soil Moisture and Vegetation Conditions during a Flash Drought–Flash Recovery Sequence over the South-Central United States, J. Hydrometeorol., 20(3), 549–562, https://doi.org/10.1175/jhm-d-18-0171.1, 2019.

Quéré, C., Andrew, R., Friedlingstein, P., Sitch, S., Hauck, J., Pongratz, J., Pickers, P., Ivar Korsbakken, J., Peters, G., Canadell, J., Arneth, A., Arora, V., Barbero, L.,

695   Bastos, A., Bopp, L., Ciais, P., Chini, L., Ciais, P., Doney, S., Gkritzalis, T., Goll,

696   D., Harris, I., Haverd, V., Hoffman, F., Hoppema, M., Houghton, R., Hurtt, G.,

697   Ilyina, T., Jain, A., Johannessen, T., Jones, C., Kato, E., Keeling, R., Klein

698   Goldewijk, K., Landschützer, P., Lefèvre, N., Lienert, S., Liu, Z., Lombardozzi,

699   D., Metzl, N., Munro, D., Nabel, J., Nakaoka, S. I., Neill, C., Olsen, A., Ono, T.,

700   Patra, P., Peregon, A., Peters, W., Peylin, P., Pfeil, B., Pierrot, D., Poulter, B.,

701   Rehder, G., Resplandy, L., Robertson, E., Rocher, M., Rödenbeck, C., Schuster,

702   U., Skjelvan, I., Séférian, R., Skjelvan, I., Steinhoff, T., Sutton, A., Tans, P., Tian,

703   H., Tilbrook, B., Tubiello, F., Van Der Laan-Luijkx, I., Van Der Werf, G., Viovy,

704   N., Walker, A., Wiltshire, A., Wright, R., Zaehle, S. and Zheng, B.: Global

705   Carbon   Budget   2018,   Earth   Syst.   Sci.   Data,   10(4),   2141–2194,

706   https://doi.org/10.5194/essd-10-2141-2018, 2018.

707 Peters, W., van der Velde, I. R., van Schaik, E., Miller, J. B., Ciais, P., Duarte, H. F.,

708   van der Laan-Luijkx, I. T., van der Molen, M. K., Scholze, M., Schaefer, K.,

709   Vidale, P. L., Verhoef, A., Wårlind, D., Zhu, D., Tans, P. P., Vaughn, B. and

710   White, J. W. C.: Increased water-use efficiency and reduced CO_2 uptake by

711   plants during droughts at a continental scale, Nat. Geosci., 11(10), 744–748,

712   https://10.1038/s41561-018-0212-7, 2018.

713 Reichstein, M., Ciais, P., Papale, D., Valentini, R., Running, S., Viovy, N., Cramer, W.,

714   Granier, A., Ogée, J., Allard, V., Aubinet, M., Bernhofer, C., Buchmann, N.,

715   Carrara, A., Grünwald, T., Heimann, M., Heinesch, B., Knohl, A., Kutsch, W.,

716   Loustau, D., Manca, G., Matteucci, G., Miglietta, F., Ourcival, J. M., Pilegaard,

K., Pumpanen, J., Rambal, S., Schaphoff, S., Seufert, G., Soussana, J. F., Sanz, M. J., Vesala, T. and Zhao, M.: Reduction of ecosystem productivity and respiration during the European summer 2003 climate anomaly: A joint flux tower, remote sensing and modelling analysis, Glob. Chang. Biol., 13(3), 634–651, https://doi.org/10.1111/j.1365-2486.2006.01224.x, 2007.

Reichstein, M., Bahn, M., Ciais, P., Frank, D., Mahecha, M. D., Seneviratne, S. I., Zscheischler, J., Beer, C., Buchmann, N., Frank, D. C., Papale, D., Rammig, A., Smith, P., Thonicke, K., Van Der Velde, M., Vicca, S., Walz, A. and Wattenbach, M.: Climate extremes and the carbon cycle, Nature, 500(7462), 287–295, https://doi.org/10.1038/nature12350, 2013.

Roman, D. T., Novick, K. A., Brzostek, E. R., Dragoni, D., Rahman, F. and Phillips, R. P.: The role of isohydric and anisohydric species in determining ecosystem-scale response to severe drought, Oecologia, 179(3), 641–654, https://doi.org/10.1007/s00442-015-3380-9, 2015.

Saleska, S. R., Didan, K., Huete, A. R. and Da Rocha, H. R.: Amazon forests green-up during 2005 drought, Science, 318(5850), 612, doi:10.1126/science.1146663, 2007.

Sippel, S., Reichstein, M., Ma, X., Mahecha, M. D., Lange, H., Flach, M. and Frank, D.: Drought, Heat, and the Carbon Cycle: a Review, Curr. Clim. Chang. Reports, 4(3), 266–286, https://doi.org/10.1007/s40641-018-0103-4, 2018.

Song, L., Luis, G., Guan, K., You, L., Huete, A., Ju, W. and Zhang, Y.: Satellite sun-induced chlorophyll fluorescence detects early response of winter wheat to

739   heat stress in the Indian Indo-Gangetic Plains, Glob. Chang. Biol., 24, 4023–

740   4037, https://doi.org/10.1111/gcb.14302, 2018.

741 Stocker, B. D., Zscheischler, J., Keenan, T. F., Prentice, I. C., Peñuelas, J. and

742   Seneviratne, S. I.: Quantifying soil moisture impacts on light use efficiency

743   across biomes, New Phytol., 218(4), 1430–1449,

744   https://doi.org/10.1111/nph.15123, 2018.

745 Stocker, B. D., Zscheischler, J., Keenan, T. F., Prentice, I. C., Seneviratne, S. I. and

746   Peñuelas, J.: Drought impacts on terrestrial primary production underestimated

747   by satellite monitoring, Nat. Geosci., 12, 274-270,

748   https://doi.org/10.1038/s41561-019-0318-6, 2019.

749 Vicente-Serrano, S. M., Gouveia, C., Camarero, J. J., Beguerá, S., Trigo, R.,

750   López-Moreno, J. I., Azorín-Molina, C., Pasho, E., Lorenzo-Lacruz, J., Revuelto,

751   J., Morán-Tejeda, E. and Sanchez-Lorenzo, A.: Response of vegetation to

752   drought time-scales across global land biomes, Proc. Natl. Acad. Sci. U. S. A.,

753   110(1), 52–57, https://doi.org/10.1073/pnas.1207068110, 2013.

754 Wang, L. and Yuan, X.: Two Types of Flash Drought and Their Connections with

755   Seasonal Drought, Adv. Atmos. Sci., 35(12), 1478–1490,

756   https://doi.org/10.1007/s00376-018-8047-0, 2018.

757 Wang, L., Yuan, X., Xie, Z., Wu, P. and Li, Y.: Increasing flash droughts over China

758   during the recent global warming hiatus, Sci. Rep., 6, 30571,

759   https://doi.org/10.1038/srep30571, 2016.

760 Wilson, K. B., Baldocchi, D. D. and Hanson, P. J.: Quantifying stomatal and

non-stomatal limitations to carbon assimilation resulting from leaf aging and drought in mature deciduous tree species, Tree Physiol., 20, 787–797, https://doi.org/10.1093/treephys/20.12.787, 2000.

Wolf, S., Eugster, W., Ammann, C., Häni, M., Zielis, S., Hiller, R., Stieger, J., Imer, D., Merbold, L. and Buchmann, N.: Erratum: Contrasting response of grassland versus forest carbon and water fluxes to spring drought in Switzerland (Environmental Research Letters (2013) 8 (035007)), Environ. Res. Lett., 9(8), https://doi.org/10.1088/1748-9326/9/8/089501, 2014.

Wolf, S., Keenan, T. F., Fisher, J. B., Baldocchi, D. D., Desai, A. R., Richardson, A. D., Scott, R. L., Law, B. E., Litvak, M. E. and Brunsell, N. A.: Warm spring reduced carbon cycle impact of the 2012 US summer drought, 113(21), 5880-5885, https://doi.org/10.1073/pnas.1519620113, 2016.

Xie, Z., Wang, L., Jia, B. and Yuan, X.: Measuring and modeling the impact of a severe drought on terrestrial ecosystem CO_2 and water fluxes in a subtropical forest, J. Geophys. Res. Biogeosciences, 121(10), 2576–2587, https://doi.org/10.1002/2016JG003437, 2016.

Xu, C., McDowell, N. G., Fisher, R. A., Wei, L., Sevanto, S., Christoffersen, B. O., Weng, E. and Middleton, R. S.: Increasing impacts of extreme droughts on vegetation productivity under climate change, Nat. Clim. Chang., https://doi.org/10.1038/s41558-019-0630-6, 2019.

Xu, H. jie, Wang, X. ping, Zhao, C. yan and Yang, X. mei: Diverse responses of vegetation growth to meteorological drought across climate zones and land

783   biomes in northern China from 1981 to 2014, Agric. For. Meteorol., 262, 1–13,

784   https://10.1016/j.agrformet.2018.06.027, 2018.

785   Yuan, W., Cai, W., Chen, Y., Liu, S., Dong, W., Zhang, H., Yu, G., Chen, Z., He, H.,

786   Guo, W., Liu, D., Liu, S., Xiang, W., Xie, Z., Zhao, Z. and Zhou, G.: Severe

787   summer heatwave and drought strongly reduced carbon uptake in Southern

788   China, Sci. Rep., 6, 18813, https://doi.org/10.1038/srep18813, 2016.

789   Yuan, W., Zheng, Y., Piao, S., Ciais, P., Lombardozzi, D., Wang, Y., Ryu, Y., Chen, G.,

790   Dong, W., Hu, Z., Jain, A. K., Jiang, C., Kato, E., Li, S., Lienert, S., Liu, S.,

791   Nabel, J. E. M. S., Qin, Z., Quine, T., Sitch, S., Smith, W. K., Wang, F., Wu, C.,

792   Xiao, Z. and Yang, S.: Increased atmospheric vapor pressure deficit reduces

793   global   vegetation   growth,   Sci.   Adv.,   5(8),   eaax1396,

794   https://doi.org/10.1126/sciadv.aax1396, 2019a.

795   Yuan, X., Ma, Z., Pan, M. and Shi, C.: Microwave remote sensing of flash droughts

796   during crop growing seasons, 17, 8196, https://doi.org/10.1002/2015GL064125,

797   2015.

798   Yuan, X., Wang, L. and Wood, E. F.: Anthropogenic intensification of southern

799   African flash droughts as exemplified by the 2015/16 season, Bull. Am. Meteorol.

800   Soc., https://doi.org/10.1175/BAMS-D-17-007.1, 2017.

801   Yuan, X., Wang, L., Wu, P., Ji, P., Sheffield, J. and Zhang, M.: Anthropogenic shift

802   towards higher risk of flash drought over China, Nat. Commun., 10(1),

803   https://doi.org/10.1038/s41467-019-12692-7, 2019b.

804   Yuan, X., Ma, F., Li, H., et al.: A review on multi-scale drought processes and predicti

805   on under global change. Trans. Atmos. Sci., 43(1), 225-237, https://doi.org/10.13

806   878/j.cnki.dqkxxb.20191105005 (in Chinese), 2020

807   Zeng, Z., Piao, S., Li, L. Z. X., Wang, T., Ciais, P., Lian, X., Yang, Y., Mao, J., Shi, X.

808   and Myneni, R. B.: Impact of Earth greening on the terrestrial water cycle, J.

809   Clim., 31(7), 2633–2650, https://doi.org/10.1175/JCLI-D-17-0236.1, 2018.

810   Zhou, S., Yu, B., Huang, Y. and Wang, G.: The effect of vapor pressure deficit on

811   water use efficiency at the subdaily time scale, Geophys. Res. Lett., 41(14),

812   5005–5013, https://doi.org/10.1002/2014GL060741, 2014.

813   Zhou, S., Bofu, Y., Huang, Y. and Wang, G.: Daily underlying water use efficiency for

814   AmeriFlux sites, J. Geophys. Res. Biogeosciences, 120, 887–902,

815   https://doi.org/10.1002/2015JG002947, 2015.

816
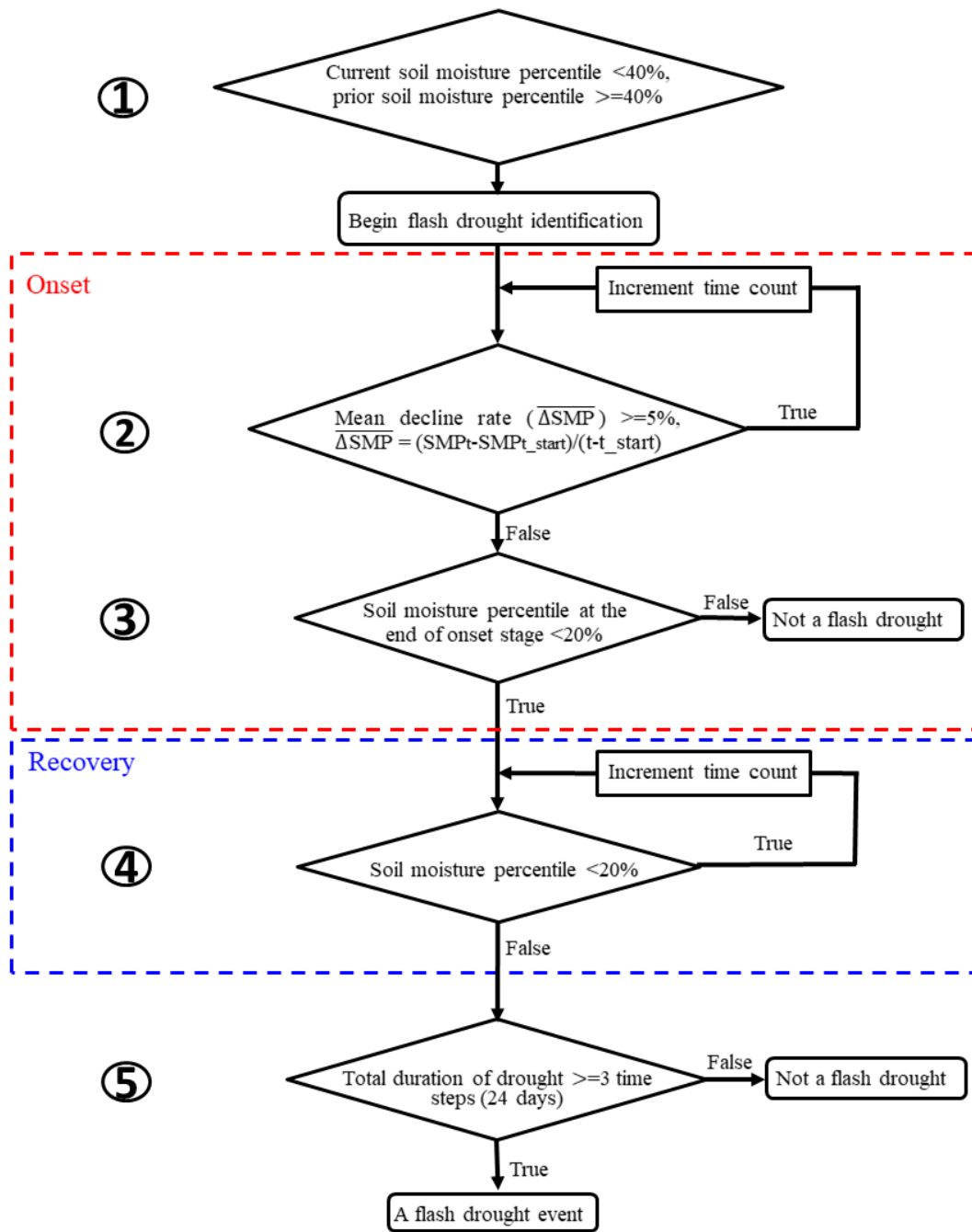
Figure 1. A flowchart of flash drought identification by considering soil moisture

decline rate and drought persistency.

819
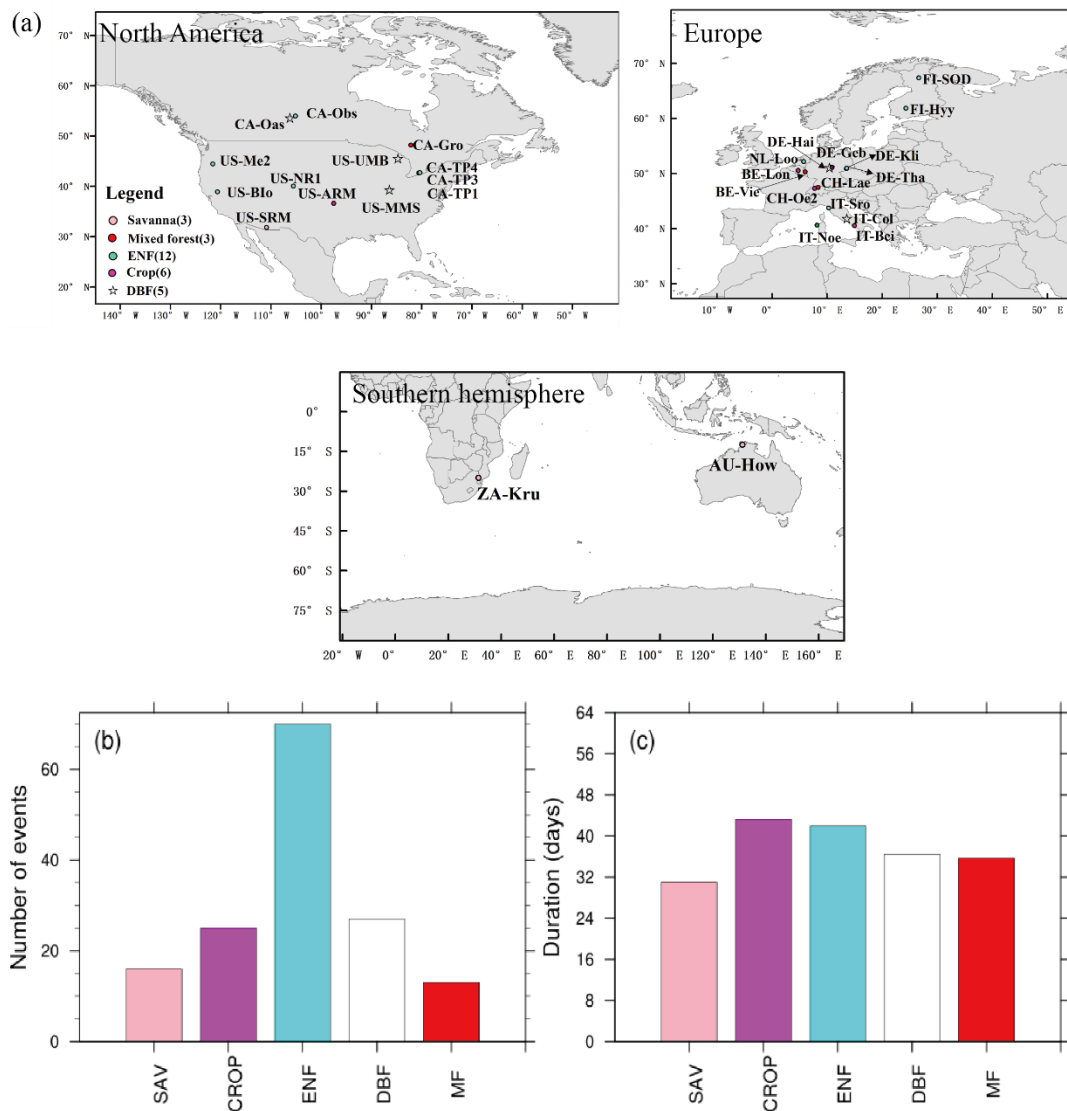
Figure 2. Global map of 29 FLUXNET sites used in this study (a) and flash drought

characteristics (b&c). (b) Total numbers (events) and (c) mean durations (days) of

flash drought events for each vegetation type during their corresponding periods (see

Table 1 for details). Different colors represent different vegetation types.

824
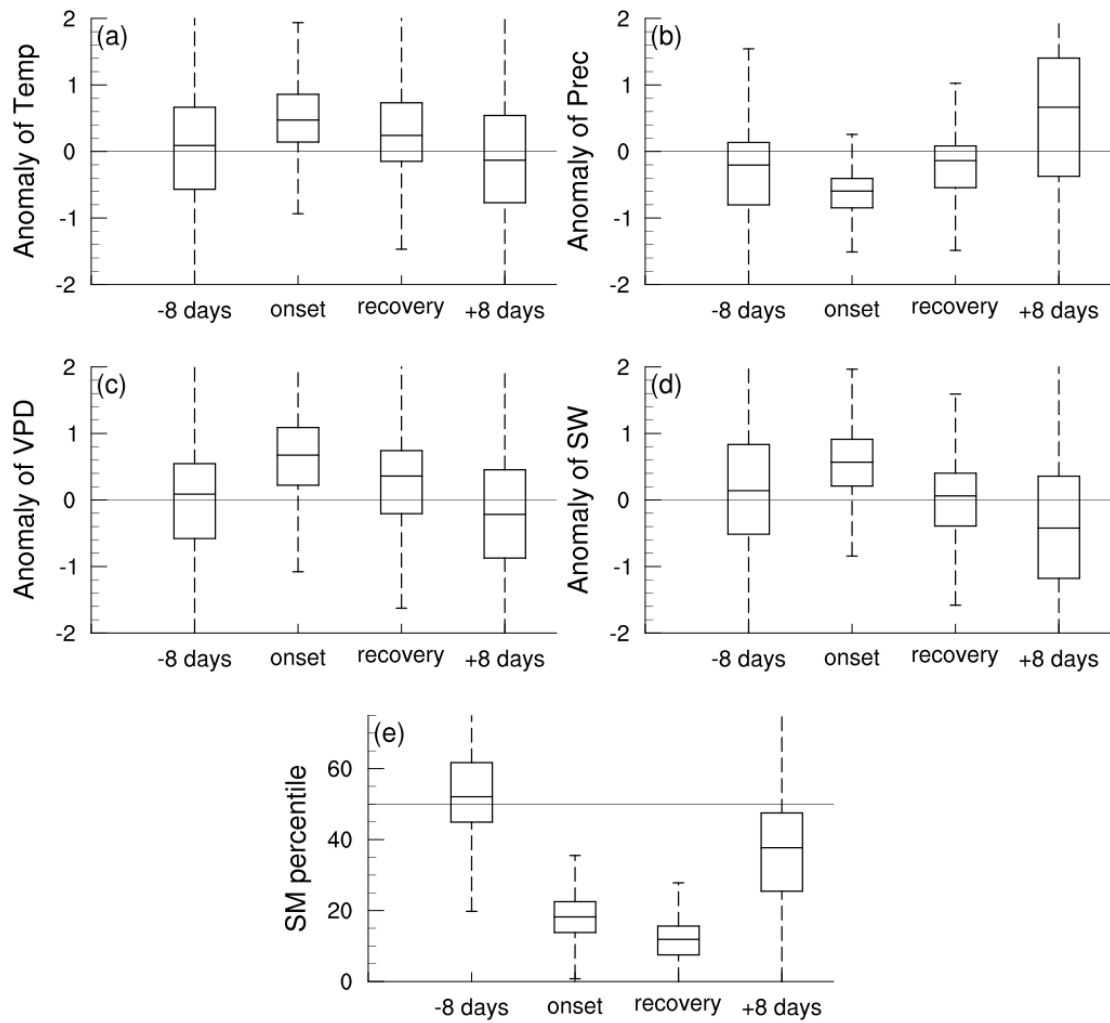
Figure 3. Standardized 8-day anomalies of (a) temperature, (b) precipitation, (c) VPD,

(d) short wave radiation (SW), and (e) soil moisture (SM) percentiles during 8 days

prior to flash drought onset, onset and recovery stages of flash drought, and 8 days

after flash drought.

829
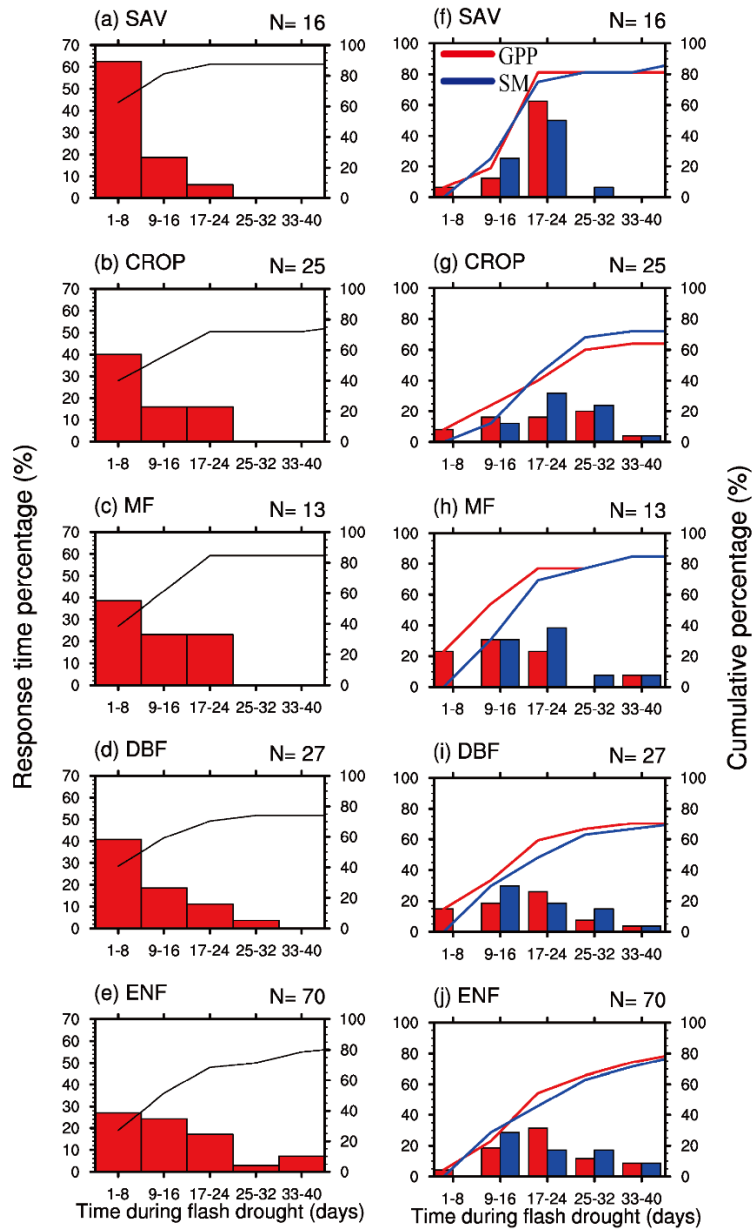
Figure 4. Percentage of the response time (days) of the first occurrence of negative

GPP anomaly (a-e), minimum GPP anomaly and minimum soil moisture percentile

(f-j) during soil moisture flash drought for different vegetation types. SAV: savanna,

CROP: rainfed cropland, MF: mixed forest, DBF: deciduous broadleaf forest and

ENF: evergreen needleleaf forest.

835
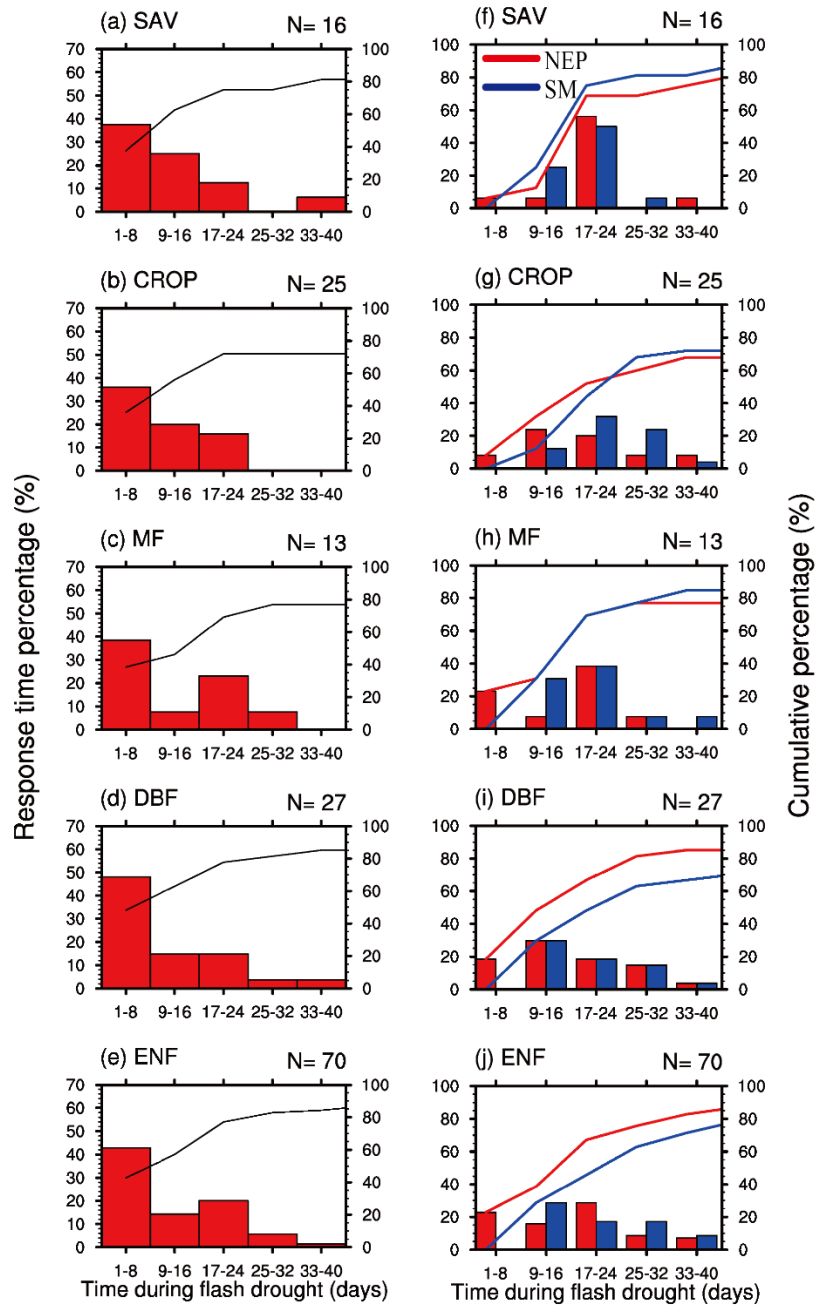
Figure 5. The same as Figure 4, but for net ecosystem productivity (NEP).

837
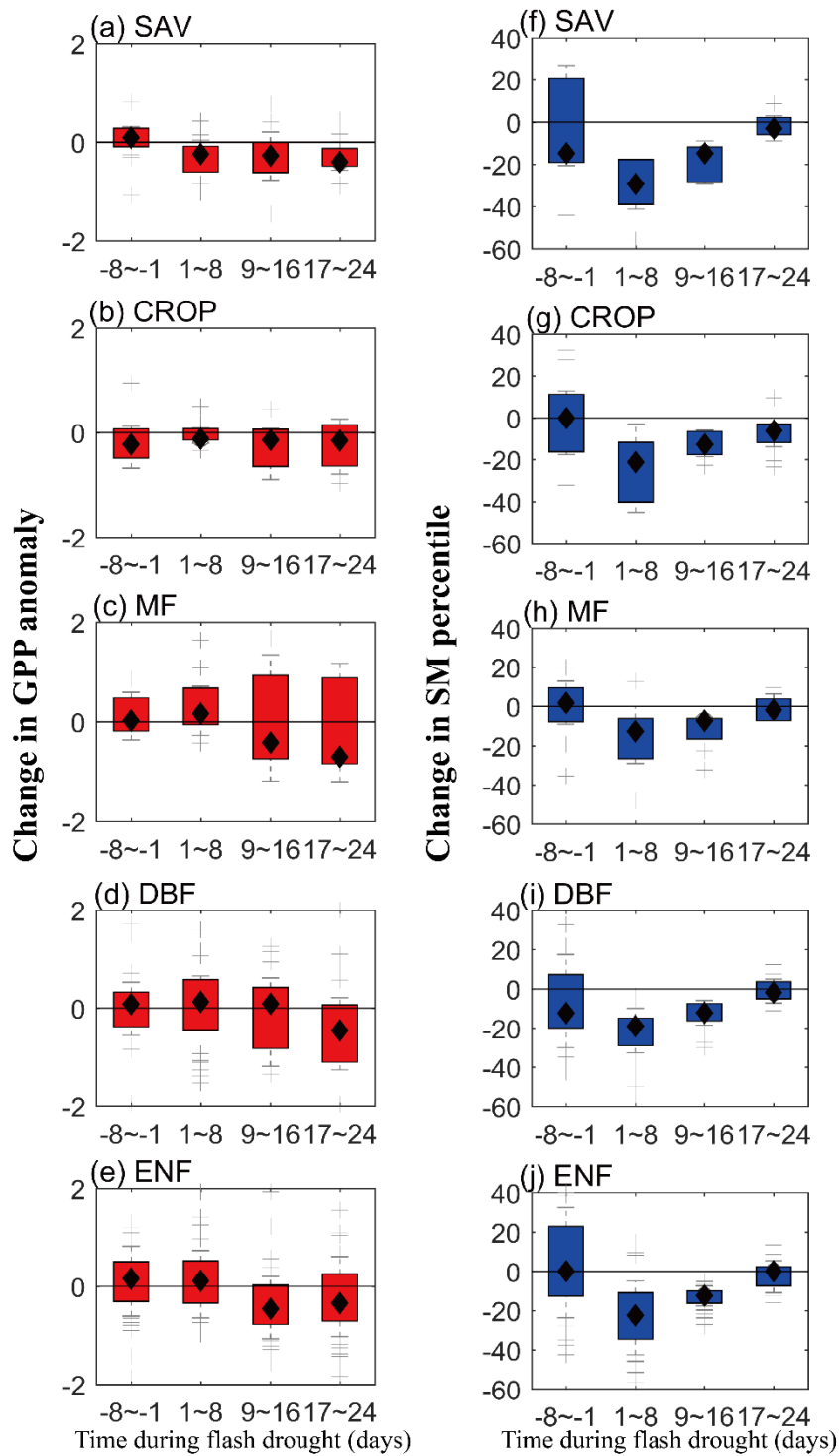
Figure 6. The temporal change rates of standardized GPP anomalies (a-e) and soil

moisture percentiles (f-j) for different vegetation types. SAV: savanna, CROP: rainfed

cropland, MF: mixed forest, DBF: deciduous broadleaf forest and ENF: evergreen

needleleaf forest.

842
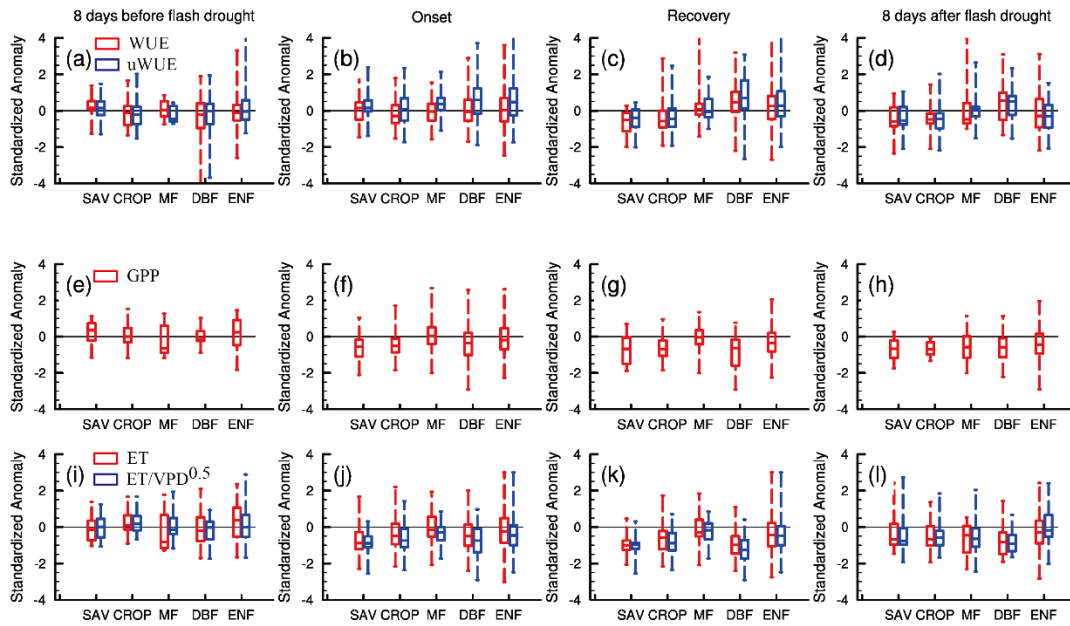
Figure 7. Standardized anomalies of water use efficiency (WUE), underlying WUE

(uWUE), GPP, ET and $ET/\sqrt{VPD}$ during 8 days before flash drought onset, onset

and recovery stages of flash drought events, and 8 days after flash drought.

846
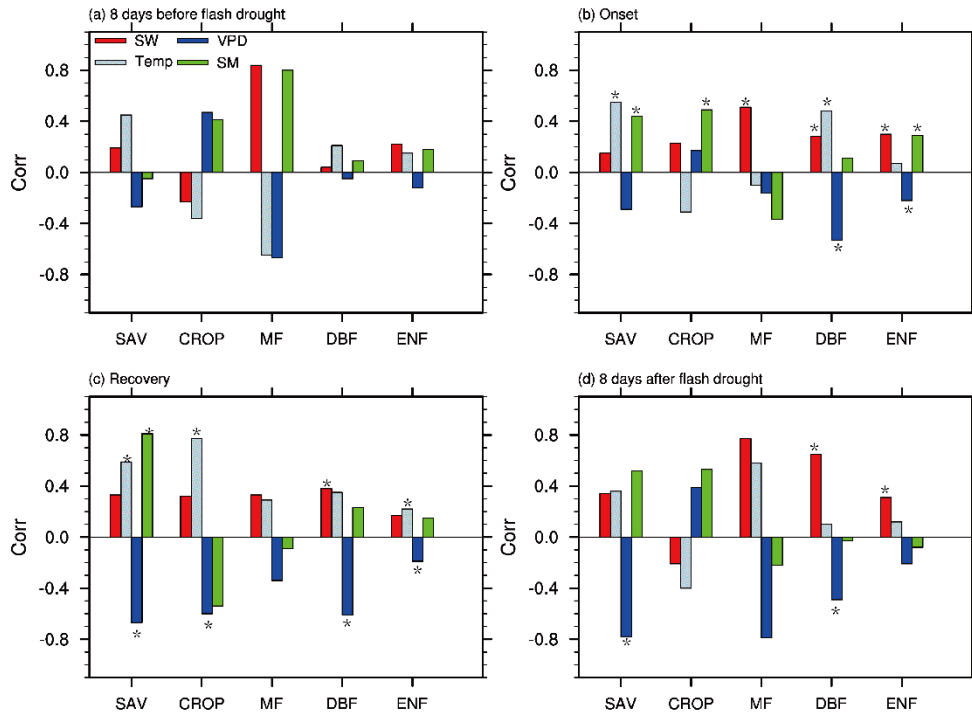
Figure 8. The partial correlation coefficients between GPP and soil moisture (SM), shortwave radiation (SW), temperature (Temp) and vapor pressure deficit (VPD) for different vegetation types including savannas (SAV), rain-fed croplands (CROP), mixed forests (MF), deciduous broadleaf forests (DBF), and evergreen needleleaf forests (ENF) during 8 days before soil moisture flash drought, onset and recovery stages and 8 days after soil moisture flash drought. * indicates the correlation is statistically significant at the 95% level.

854 **Table 1.** Locations, vegetation types and data periods of Flux Tower Sites used in this

855 study. WSA: woody savanna; CROP: cropland; EBF: evergreen broadleaf forests; MF:

856 mixed forest; DBF: deciduous broadleaf forest; ENF: evergreen needleleaf forest;

857 GRA: grassland; SAV: savanna.

station	lat	lon	IGBP	period
AU-How	-12.49	131.15	WSA	2002-2014
BE-Lon	50.55	4.75	CROP-rainfed	2004-2014
BE-Vie	50.31	6.00	MF	1997-2014
CA-Gro	48.22	-82.16	MF	2004-2013
CA-Oas	53.63	-106.20	DBF	1996-2010
CA-Obs	53.99	-105.12	ENF	1999-2010
CA-TP1	42.66	-80.56	ENF	2002-2014
CA-TP3	42.71	-80.35	ENF	2002-2014
CA-TP4	42.71	-80.36	ENF	2002-2014
CH-Lae	47.48	8.37	MF	2005-2014
CH-Oe2	47.29	7.73	CROP-rainfed	2004-2014
DE-Geb	51.10	10.91	CROP-rainfed	2001-2014
DE-Hai	51.08	10.45	DBF	2000-2012
DE-Kli	50.89	13.52	CROP-rainfed	2005-2014
DE-Tha	50.96	13.57	ENF	1997-2014
FI-Hyy	61.85	24.29	ENF	1997-2014
FI-Sod	67.36	26.64	ENF	2001-2014
IT-Bci	40.52	14.96	CROP-irrigated	2005-2014
IT-Col	41.85	13.59	DBF	2005-2014
IT-Sro	43.73	10.28	ENF	2000-2012
NL-Loo	52.17	5.74	ENF	1999-2013
US-ARM	36.61	-97.49	CROP-rainfed	2003-2013
US-Blo	38.90	-120.63	ENF	1998-2007
US-Me2	44.45	-121.56	ENF	2002-2014
US-MMS	39.32	-86.41	DBF	1999-2014
US-NR1	40.03	-105.55	ENF	2002-2014
US-SRM	31.82	-110.87	WSA	2004-2014
US-UMB	45.56	-84.71	DBF	2002-2014
ZA-Kru	-25.02	31.50	SAV	2000-2010